applied sciences

MDPI

Article

Direct Conversion of Human Fibroblasts into Osteoblasts Triggered by Histone Deacetylase Inhibitor Valproic Acid

Hyeonjin Cha [1,†], Jaeyoung Lee [1,†], Hee Ho Park [2,*] and Ju Hyun Park [1,*]

[1] Department of Medical Biomaterials Engineering, Kangwon National University, Chuncheon-si, Gangwon-do 24341, Korea; hyeon_j03@kangwon.ac.kr (H.C.); leejy5999@kangwon.ac.kr (J.L.)
[2] Department of Biotechnology and Bioengineering, Kangwon National University, Chuncheon-si, Gangwon-do 24341, Korea
* Correspondence: hhpark@kangwon.ac.kr (H.H.P.); juhyunpark@kangwon.ac.kr (J.H.P.); Tel.: +82-33-250-6271 (H.H.P.); +82-33-250-6566 (J.H.P.)
† These authors contributed equally to this work.

Received: 25 September 2020; Accepted: 19 October 2020; Published: 21 October 2020

Abstract: The generation of functional osteoblasts from human somatic cells could provide an alternative means of regenerative therapy for bone disorders such as osteoporosis. In this study, we demonstrated the direct phenotypic conversion of human dermal fibroblasts (HDFs) into osteoblasts by culturing them in osteogenic medium supplemented with valproic acid (VPA), a histone deacetylase (HDAC) inhibitor. HDFs cultured with the VPA in osteogenic medium exhibited expression of alkaline phosphatase and deposition of mineralized calcium matrices, which are phenotypical characteristics of functional osteoblasts. They also expressed osteoblast-specific genes such as alkaline phosphatase, osteopontin, and bone sialoprotein, which demonstrated their direct conversion into osteoblasts. In addition, co-treatment with VPA and a specific inhibitor for activin-like kinase 5 (ALK5i II) had a synergistic effect on direct conversion. It is considered that the inductive effect of VPA on the conversion into osteoblast-lineage is due to the opening of the nucleosome structure by HDAC inhibitor, which facilitates chromatin remodeling and cellular reprogramming. Our findings provide a novel insight into the direct conversion of human somatic cells into transgene-free osteoblasts with small chemical compounds, thus making bone regeneration using cellular reprogramming strategy more clinically feasible.

Keywords: direct conversion; osteoblast; histone deacetylase inhibitor; valproic acid; inhibitor for activin-like kinase 5

1. Introduction

Transcription factors (also known as reprogramming factors) are proteins that can control the transcriptional regulation of genetic information by binding to specific DNA sequences [1,2]. In 2006 and 2007, ground-breaking research by Takahashi and Yamanaka demonstrated that forced expression of a set of transcription factors such as c-Myc, Oct3/4, Sox2, and Klf-4, enable reprogramming of somatic cells into induced pluripotent stem cells (iPSCs) that have the ability to self-renew and pluripotency [3,4]. Over the past decade, numerous studies have been conducted to reprogram and convert somatic cells into targeted phenotypes by using various approaches including genetic manipulation, biomaterials, growth factors, small molecules, and cocktails thereof. The "direct conversion" (also known as direct reprogramming) of somatic cells to another differentiated lineage by introducing a combination of transcription factors, is considered to be a more promising strategy, and it involves bypassing the intermediate pluripotent stage [5]. The ability of somatic cells to transdifferentiate into tissue-specific

progeny without going through the time-consuming pluripotent generating step is considered to be a promising strategy for regenerative medicine in clinical settings. These direct conversions include fibroblasts into cardiomyocytes [6,7], neurons [8–11], chondrocytes [12–14] and more in other lineages. However, the process of direct conversion in vitro is still relatively slow and not very efficient, which hinders research on the mechanisms of reprogramming and progress in clinical applications.

Approaches that use small molecules for the direct conversion of somatic cells are highly desirable, and it is thought that small molecules can significantly improve their use in therapeutic applications. Using small molecules for reprogramming and conversion of cell lineage is an exciting area of research and this has helped to identify small molecules that promote self-renewal [15–19], differentiation of stem cells [20–24], and reprogramming, for example, in the induction of stem cells [25–29] and direct conversion of somatic cells [30–32]. It has been shown that small molecules can promote osteogenesis and bone regeneration [21,33–36].

Mesenchymal stem cells (MSCs) are multipotent stem cells that have the ability to differentiate into various cell types, such as adipocyte, myoblasts, chondrocytes, and osteoblasts [37,38]. Among these, osteoblasts play a pivotal role in bone generation, and produce various types of bone extracellular materials, such as type I collagen, osteopontin (OPN), osteocalcin (OCN), and bone sialoprotein (BSP) [39]. Osteoblast differentiation is controlled by various transcription factors such as Runt-related transcription factor 2 (Runx2) [40,41], Osterix [42,43], and distal-less homeobox 5 (Dlx5) [44,45]. However, a decline in the number of osteoblasts with respect to osteoclasts can cause an imbalance between bone formation and resorption, and can subsequently lead to pathological conditions such as osteoporosis [46], and bone degeneration-associated tumors such as multiple myeloma [47]. Such regeneration of bone tissue for therapies represents a serious health problem, and remains a significant challenge in terms of clinical feasibility. This is because the available therapeutic approaches are often accompanied by slow treatment, poor efficiency, pain, risk of infection, immunogenicity problems, and tumorigenesis after cell implantation [48]. Therefore, the development of transgene-free therapeutic approaches for bone repair is urgently needed. In this study, we hypothesized that VPA could be used to enhance the differentiation efficiency of MSCs, and it could also improve the efficiency of reprogramming somatic cells to osteoblasts.

Herein, we report the direct conversion of human fibroblasts into osteoblasts by using a transgene-free approach and the use of osteoblast-promoting factors: histone deacetylase (HDAC) inhibitor and tumor growth factor-β receptor (TGF-β R) inhibitor. We assessed the ability of the synergistic effect to promote osteogenesis after co-treatment with valproic acid (VPA), a HDAC inhibitor, and a specific inhibitor for activin-like kinase 5 (ALK5i II), a TGF-β R inhibitor. We performed an experimental analysis at two time points for observation of the early stage (day 16) and the late stage (day 24) markers [39]. It is anticipated that this highly efficient synergistic strategy, which does not involve the transgene, may be useful for regenerative therapy against a variety of human diseases. If sufficient efficiency can be achieved with a small molecule-based approach, then such cell-based therapies could be beneficial in clinical settings for the generation of bone and repair of bone defects.

2. Materials and Methods

2.1. Reagents and Cell Culture

VPA (Sigma Aldrich, St. Louis, MI, USA) was dissolved in distilled water (DW) and stored at −70 °C until use. VPA was diluted in the medium to meet the working concentration used in the experiment. Human dermal fibroblasts isolated from neonatal foreskin (HDFs, #C-004-5C, Thermo Fisher Scientific, Waltham, MA, USA) was maintained in Dulbecco's Modified Eagle's Medium (DMEM, Hyclone, Locan, UT, USA) supplemented with 10% fetal bovine serum (FBS, Welgene, Daejeon, Korea), 100 U/mL penicillin and 100 µg/mL streptomycin (Thermo Fisher Scientific) in a 5% CO_2 humidified incubator at 37 °C. We assumed that only HDFs were present in the vial from the provider (i.e., there

were no stem-like cells in the vial). When the confluence reached 80%, HDFs were sub-cultured with a split ratio of 1:6. HDFs used in this study were under passage 7 in all experimental steps.

2.2. In Vitro Differentiation of HDFs

HDFs were seeded in a 24-well plate at a density of 1×10^4 cells/cm^2 and incubated for 24 h in complete medium. For osteogenic differentiation, the medium was replaced with fresh complete medium (DMEM supplemented with 10% FBS, 100 U/mL penicillin and 100 µg/mL streptomycin) supplemented with 10 mM β-glycerol phosphate, 50 µg/mL ascorbic acid, and 100 nM dexamethasone (osteogenic medium, O.M.). All supplements used in the osteoblast differentiation were purchased from Sigma Aldrich. For differentiation, osteogenic medium supplemented with VPA was replaced every 2 days and incubated for a further 24 days.

2.3. Cytotoxicity Test (MTT Assay)

Cytotoxicity testing was performed to evaluate the toxicity to VPA and ALK5i II. First, HDF was seeded in a 96-well plate. The next day, after washing with PBS, the chemicals were treated with various VPA concentrations in complete medium. Then, MTT (Sigma Aldrich) solution was added to each well every 24, 48 h, and 72 h. (final concentration 1 mg/mL) and incubated further at 37 °C for 4 h. After removing the supernatant, DMSO was added, and the absorbance was measured at 540 nm using a microplate reader.

2.4. Alkaline Phosphatase (ALP) Staining

To analyze the degree of differentiation of HDFs into osteoblasts, staining was performed on day 16 after differentiation. After fixing for 15 min with 4% paraformaldehyde (PFA), it was washed 3 times with phosphate-buffer saline (PBS). The Alkaline Phosphatase Staining kit II (Stemgent, Lexington, MA, USA) was used to visualize the ALP activity. Staining was performed according to the protocol provided by the manufacturer.

2.5. Detection of Calcium Deposits (Mineralization)

In the case of Alizarin Red S (ARS) staining, 4% PFA was fixed for 15 min and then washed 3 times with DW. Next, the mineralized part was stained for 10 min in the dark using 2% ARS (Sigma Aldrich) solution, washed with DW and then analyzed. Von Kossa staining was performed in the same manner as outlined above and washed 3 times with DW. Next, the mineralized part was confirmed using the Von Kossa Staining kit (Abcam, Cambridge, MA, USA). Staining was performed according to the protocol provided with the kit. All stained images were analyzed under a microscope.

2.6. Quantification of ARS

To quantify the calcium deposits, the stained plates were analyzed according to the protocol provided in the Alizarin Red Staining Quantification Assay kit (ScienCell, Carlsbad, CA, USA). Briefly, 200 µL of 10% acetic acid was added to each stained well and shaken at room temperature for 30 min. After heating the dissolved stain at 85 °C for 10 min, it was transferred to ice and cooled for 5 min. Following centrifugation, the supernatant was transferred to a new tube, and 10% ammonium hydroxide was added for neutralization. Finally, the absorbance was measured at 405 nm using a spectrophotometer.

2.7. Quantitative Real-Time Polymerase Chain Reaction (qPCR)

Total RNA was obtained from HDFs after differentiation using a Ribospin™ total RNA Purification kit (Gene All Biotechnology, Seoul, Korea). Next, cDNA was synthesized using TOPscript™ RT PCR DryMIX (Enzynomics, Daejeon, Korea). Three types of osteoblast gene-specific primers (Applied Biosystems, Foster City, CA, USA) Osteopontin (Hs00960942_m1), ALP (Hs00758162_m1), and BSP

(Hs00913377_m1) were used to analyze the degree of osteoblast differentiation at the gene level. Real time PCR was performed using Taqman™ Fast Advanced Master Mix (Applied Biosystems) and Eco Real-Time PCR System (Illumina, San Diego, CA, USA). The expression level of each gene was normalized by glyceraldehyde 3-phosphate dehydrogenase (GAPDH, Hs99999905_m1) as endogenous control, and relative fold change compared to control group was calculated by the ΔΔCt ($RQ = 2^{-[\Delta Ct\ sample - \Delta Ct\ control]}$).

2.8. Statistical Analysis

All values are written as the mean ± S.D. All quantitative data are obtained from triplicate samples from experiments that were performed several times. The statistical significance was determined by Student's *t*–test, one-way analysis of variance (ANOVA) followed by Tukey's post hoc test, and Welch's ANOVA followed by Games-Howell post hoc test. $p < 0.05$ was considered statistically significant.

3. Results

3.1. VPA Increases Osteoblast-Like Phenotype of HDFs

Some small chemicals have been shown to enhance the differentiation of stem cells to other lineages [20–24], some increase the reprogramming and induction of stem cell phenotypes [25–29], while others promote the direct conversion of somatic cells into other lineages [30–32]. Among these, VPA was selected and tested as to whether it induces osteoblast-like phenotypes in HDFs. It has been widely reported that small molecule VPA promotes reprogramming via inhibition of HDAC activity, thus causing hyperacetylation of histones [26,49–51].

HDFs were cultured in osteogenic medium supplemented with VPA for 16 days, and the ALP activities were analyzed (Figure 1a). As the concentration of VPA increased to 2 mM, there was an increase in ALP activity. HDFs were cultured in osteogenic medium supplemented with VPA for 24 days, and stained with ARS to estimate calcium deposition (Figure 1b). VPA at a concentration of 2 mM induced relatively large amounts of calcium deposition, whereas VPA at 1 mM induced some visible amount of calcium deposition compared to the osteogenic medium alone (Figure 1b). Then we quantified the ARS fold change after the treatment of VPA. It was clearly shown that the amount of ARS-stained calcified matrices increased according to VPA treatment in a dose-dependent manner (Figure 1c). Hence, the results demonstrated the potential of VPA as a potent small molecule for inducing osteoblastic conversion.

3.2. Growth Inhibitory Effect of VPA on HDFs

The cellular toxicity of VPA was measured by observing the morphological changes in the HDFs (Figure 2a). HDFs have a large, flat, and elongated shape and are characterized by processes extending out from the ends of the cell body giving bipolar or multipolar morphology. No apparent morphological differences were observed when VPA was treated in the 0–2 mM range. However, when the concentration of VPA was increased to 4 mM, a longer cellular body and thinner sprouting were observed. Nevertheless, no observable cell death was seen at high concentration, which indicates that VPA is not cytotoxic but it may be a growth inhibitor.

In addition, the cellular toxicity of VPA was measured on HDFs using MTT assay (Figure 2b). No significant decrease in the cell viability was observed after 24 h exposure with VPA in the 0–4 mM range (Figure 2b, left panel). A slight decrease in the MTT reduction was observed after 48 h exposure with VPA at 4 mM (Figure 2b, middle panel). Similarly, as the exposure time period was increased to 72 h, a decrease in the cell viability was observed in all concentrations (1, 2, and 4 mM VPA), indicating the time-dependent growth inhibitory property of VPA (Figure 2b, right panel). As 4 mM VPA resulted in high growth inhibition, we then continued the experiments with less than 2 mM VPA. It was noticeable that with prolonged exposure to VPA, the growth inhibition of the fibroblasts went from 80% on day 3 down to 40% on day 16 (Figure 2b,c).

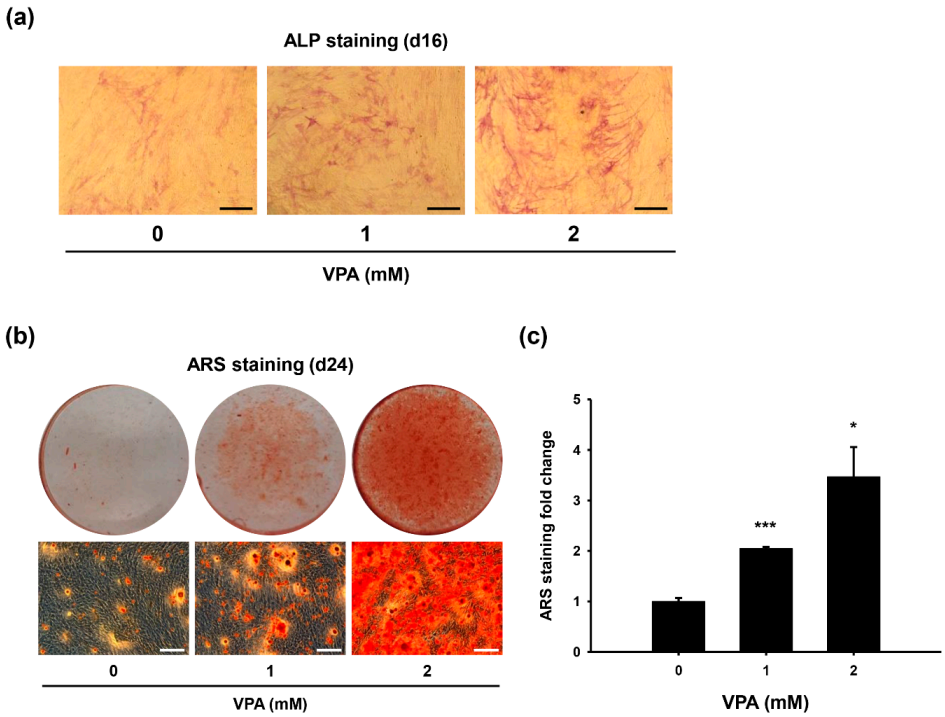

Figure 1. Valproic acid (VPA) promotes osteogenesis via inhibition of histone deacetylase (HDAC). (**a**–**c**) Human dermal fibroblasts (HDFs) were cultured in the osteogenic medium supplemented with VPA as indicated. (**a**) After culturing for 16 days, cells were stained with alkaline phosphatase (ALP). Scale bar, 200 μm. (**b**) After culturing for 24 days, calcium deposition was assessed by Alizarin Red S (ARS) staining. Scale bar, 100 μm. (**c**) Quantified ARS fold change after the treatment of VPA. Error bars indicate the standard deviation (n = 3 per group) and statistical significance was determined using Welch's ANOVA with a Games-Howell post hoc test in comparison to the non-treated control, * $p < 0.05$, *** $p < 0.005$.

3.3. Gene Expression of Osteogenic Markers in HDFs Supplemented with VPA

HDFs were cultured in osteogenic medium supplemented with VPA for 16 or 24 days, and analyzed for the expression of osteogenic markers (Figure 3). As the concentration of VPA increased to 2 mM, there was an increase in the mRNA level of alkaline phosphatase (ALP), an early osteogenic marker, at Day 16 (Figure 3a). Similarly, when the concentration of VPA was increased to 2 mM, an increase in the mRNA level of osteopontin (OPN) and bone sialoprotein (BSP), both of which are late osteogenic markers, was observed at Day 24 (Figure 3b,c). The results demonstrate that VPA induces all early and late osteogenic differentiation-related gene (ALP, OPN, BSP) expression patterns during direct conversion of HDFs cells in vitro.

3.4. Co-Treatment of VPA and Specific Inhibitor for Activin-Like Kinase 5 (ALK5i II) Enhances Osteoblast-Like Phenotypes of HDFs

To further enhance the efficiency of the direct conversion, ALK5i II, a TGF-β R inhibitor was co-supplemented with VPA. HDFs were cultured in osteogenic medium co-supplemented with VPA and ALK5i II for 24 days, and stained with ARS to observe the calcium deposition efficiency (Figure 4a). VPA alone at 2 mM concentration induced relatively large amounts of calcium deposition, whereas VPA alone at 1 mM induced little calcium deposition, similar to the osteogenic medium alone. However, when ALK5i II and VPA were used for co-treatment, synergistic effects were shown on the direct conversion into osteoblasts. Treatments with 1 mM VPA and 100 nM ALK5i II induced relatively large amounts of calcium deposition that were similar to the 2 mM VPA alone.

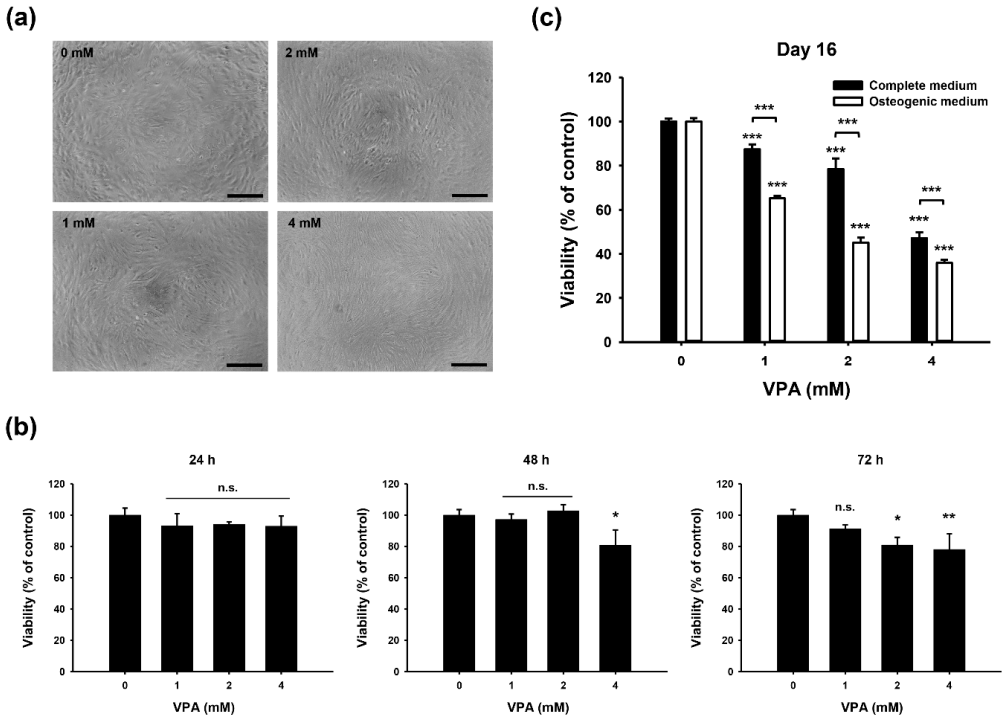

Figure 2. Cytotoxicity of VPA on HDFs. (**a**,**b**) HDFs were cultured in the osteogenic medium supplemented with VPA as indicated. (**a**) Morphologies were observed in cells treated with VPA for 72 h. The concentration of VPA is indicated in the upper left of each image. Scale bar, 200 μm. (**b**) Cell viability was measured by the MTT assay after VPA treatment for 24, 48 h, or 72 h, respectively. Error bars indicate the standard deviation (n = 3 per group) and statistical significance was determined using one-way ANOVA with Tukey's post hoc test in comparison to the non-treated control, * $p < 0.05$, ** $p < 0.01$, n.s. = not significant. (**c**) Cell viability was measured by the MTT assay after VPA treatment in complete media or osteogenic media for 16 days, respectively. Error bars indicate the standard deviation (n = 3 per group) and statistical significance was determined using one-way ANOVA with Tukey's post hoc test in comparison to the non-treated control, *** $p < 0.005$. Statistical significance was determined using Student's t-test in the comparison between groups cultured in complete medium and osteogenic medium at the same VPA concentration, *** $p < 0.005$.

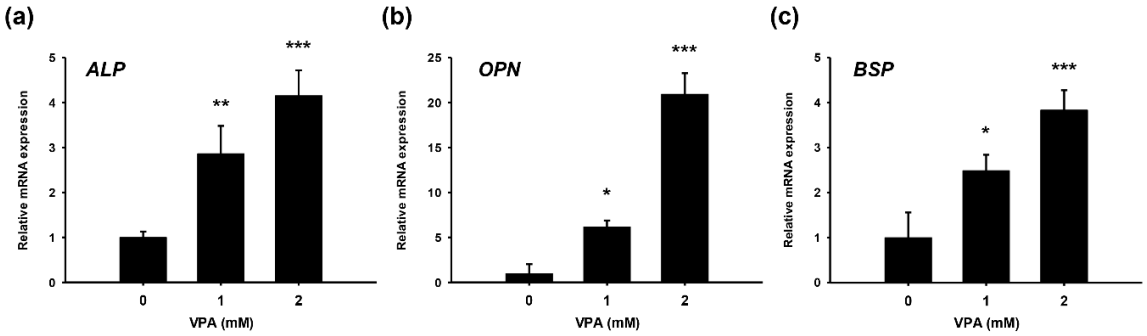

Figure 3. Gene expression of osteogenic markers in HDFs supplemented with VPA. (**a**–**c**) Quantitative real time-PCR was used to determine mRNA levels of (**a**) alkaline phosphatase (ALP) on Day 16, (**b**) osteopontin (OPN), (**c**) bone sialoprotein (BSP) on Day 24 after HDFs were treated with the osteogenic medium supplemented with VPA as indicated. Error bars indicate the standard deviation (n = 3 per group) and statistical significance was determined using one-way ANOVA with Tukey's post hoc test in comparison to the non-treated control, * $p < 0.05$, ** $p < 0.01$, *** $p < 0.005$.

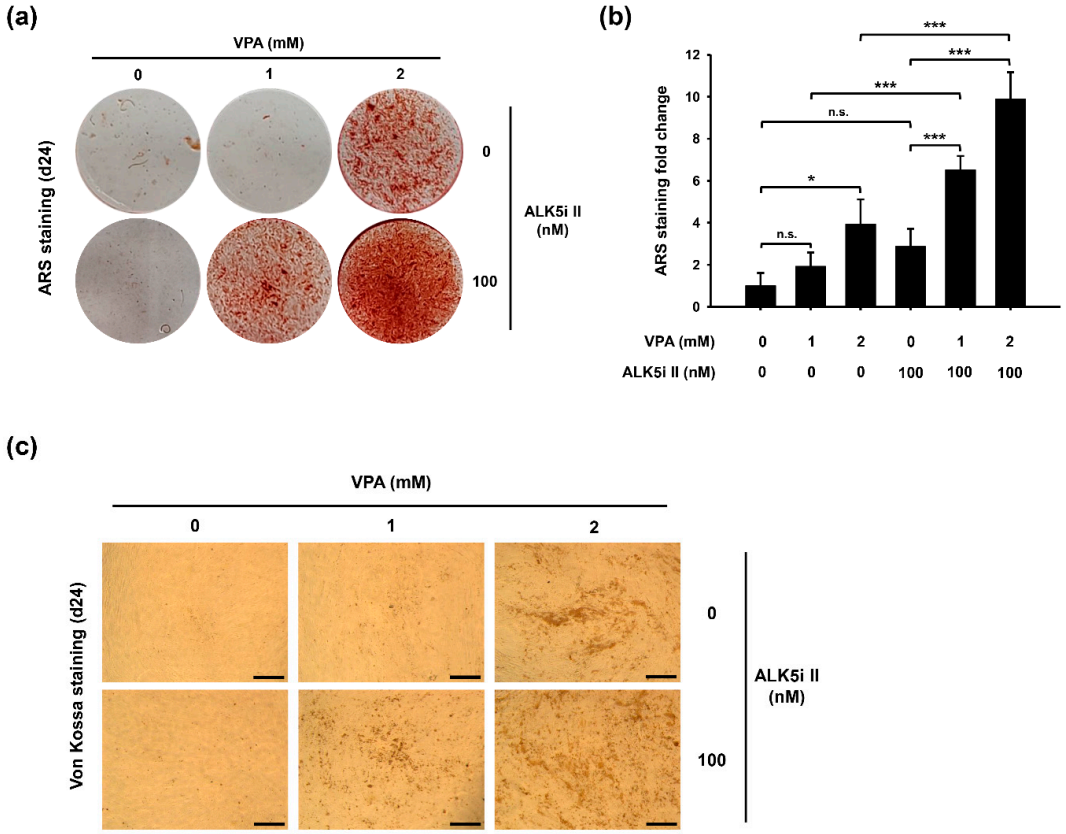

Figure 4. Osteoblast-like phenotypes were induced in HDFs cultured with VPA and specific inhibitor for activin-like kinase 5 (ALK5i II). (**a**–**c**) HDFs were cultured in the osteogenic medium supplemented with VPA and ALK5i II as indicated. (**a**) After culturing for 24 days, calcium deposition was assessed by ARS staining. (**b**) Quantified ARS fold change after the co-treatment. Error bars indicate the standard deviation (n = 3 per group) and statistical significance was determined using one-way ANOVA with Tukey's post hoc test, * $p < 0.05$, *** $p < 0.005$, n.s. = not significant. (**c**) After culturing for 24 days under co-treatment conditions, calcium deposition was assessed by Von Kossa staining. Scale bar, 200 µm.

Then we quantified the ARS fold change after the co-treatment with VPA and ALK5i II (Figure 4b). When the cells were co-treated with 100 nM AKL5i II, the amount of calcium deposition was more than 3-fold and 2.5-fold higher with VPA at 1 mM and 2 mM, respectively, compared to treatment with the same concentration of VPA only. Dose-dependent calcium phosphate deposition was observed as the concentration of VPA increased in both the single (VPA alone) or co-supplemented (VPA and ALK5i II) groups.

Next, HDFs were cultured in osteogenic medium co-supplemented with VPA and ALK5i II for 24 days, and stained with Von Kossa to understand the mineralization effects and further support the calcium deposition efficiency demonstrated by ARS staining (Figure 4c). Similar to ARS staining, VPA alone at 2 mM concentration induced a relatively large amount of calcified matrices, whereas VPA alone at 1 mM induced a small amount of calcification s, which was similar to the osteogenic medium alone. However, when we co-supplemented with 2 mM VPA and 100 nM ALK5i II, this induced a relatively large amount of calcified matrices, whereas 1 mM VPA and 100 nM ALK5i II induced a relatively large amount of calcification that was similar to the 2 mM VPA alone. Hence, these results demonstrated that when VPA is used in conjunction with ALK5i II, the potential of VPA as a potent small molecule in osteoblastic conversion is further increased.

4. Discussion

Histone modification and DNA methylation constitute major mechanisms that are responsible for epigenetic regulation of gene expression during development and differentiation [52–54]. Among various histone modifications, acetylation is known to impact the physical properties of chromatin and there is significant evidence that histone acetylation is important in nucleosome assembly and chromatin folding [55]. It was shown that lysine charge neutralization achieved through histone tail acetylation reduces inter-nucleosomal interactions, and results in the unfolding of the chromatin fiber. It is now widely acknowledged that acetylation promotes the opening of the chromatin structure by interfering with the interactions between nucleosomes and releasing the histone tails from the linker DNA.

HDAC inhibitors are small molecules that can promote either self-renewal, differentiation, or reprogramming of cells under certain conditions. In the past decade, due to their role in epigenetic regulation, gene expression profiles, and signal transduction pathways, HDAC inhibitors have been widely used to convert the state of cells into other lineages. It has been reported that VPA, which is a HDAC inhibitor, promotes chromosomal remodeling and maintains acetylated histones as an "open form" of the chromatin structure by acting as an inhibitor of HDAC [26,49–51], thereby enhancing reprogramming of somatic cells into iPSCs and other lineages. Previous reports have shown that treatment of VPA arrests cellular growth [51,56]. Similar to the effect of VPA in osteogenic medium, increasing the concentration of VPA in complete medium showed increased growth inhibition of cells (Figure 2c). However, the extent of the growth inhibition was less profound in complete medium than in osteogenic medium, which is considered to be because the fibroblasts in osteogenic medium supplemented with VPA underwent a shift from a proliferative state to a cellular reprogramming process. In addition, treatment of VPA in complete medium resulted in no observable difference in cellular morphology and calcium deposition (data not shown), whereas significant changes were observed in osteogenic medium with VPA (Figure 1b). These results suggest that osteogenic medium is a key factor for the direct conversion of fibroblasts into osteogenic lineage, and VPA acts as an enhancer in the reprogramming process.

Previously, it has been shown that VPA promotes cell fate determination via activation of the ERK pathway [57] and suppression of STAT3 and HDAC3 pathways [58]. In particular, VPA was used as a substitute for c-myc in reprogramming [26]. The treatment of VPA increased the number of iPSC colonies by more than 50-fold, and the reprogrammed iPSCs resembled ESCs with regard to their morphology, pluripotency and gene expression profiles [26]. Recently, it was demonstrated that VPA is a potential inducer of osteogenesis in mouse mesenchymal stem cells (MSCs) [59]. Molecular analysis showed upregulation of Runx2, osteoblast-related differentiation markers, and bone-related transcription factors in VPA-treated mouse MSCs. In vitro analysis using ARS and Von Kossa staining results showed an increase in the deposition of calcium phosphate in VPA-treated mouse MSCs and confirmed osteoblast differentiation and mineralization. It is considered that VPA sets somatic cells in a transition state before they continue and complete the reprogramming process. In addition, it has been reported that VPA promotes osteogenic differentiation of bone marrow-derived mesenchymal stem cells (BMSCs) by alleviating the adverse effect of glucocorticoids on BMSC proliferation, apoptosis and osteogenic differentiation [60]. In a previous study, expression levels of Runx2 and other osteogenic markers were analyzed as early markers for the differentiation of MSCs into osteogenic lineage [61]. It was noticeable that Runx2 and other osteogenic markers were increased simultaneously. Accordingly, we selected ALP as the early stage marker and provided the staining analysis in Figure 1a and gene expression analysis in Figure 3a. Based on the previous finding, it was expected that the Runx2 level would also increase along with ALP level. Taken together, it was hypothesized that that small molecule VPA promotes the induction of osteoblasts and mineralization of calcium matrices via formation of hyper-acetylated histones through inhibition of HDAC activity (Figure 5).

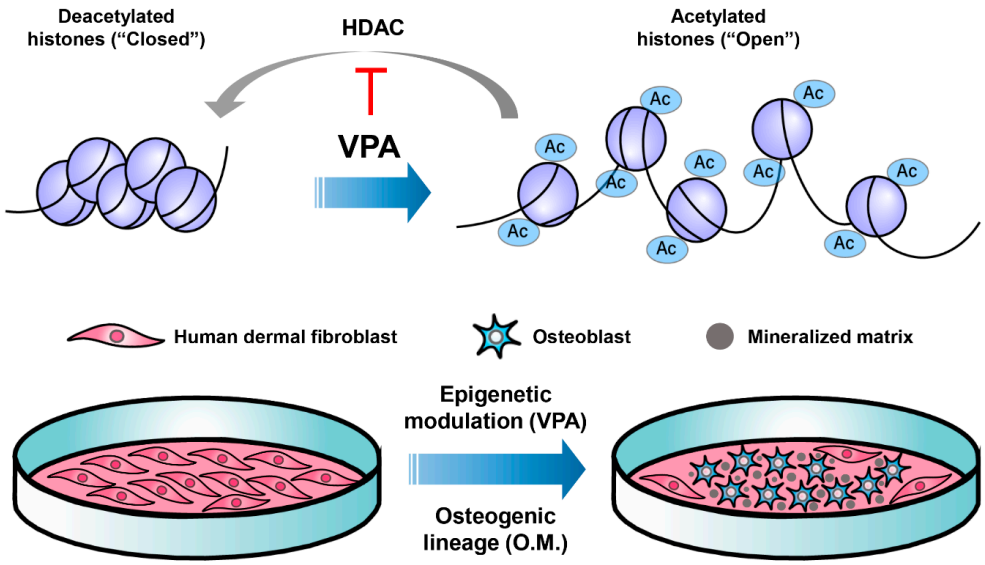

Figure 5. Schematic illustration of increased direct conversion efficiency of somatic cells into osteoblasts and mineralization by supplementation of VPA in osteogenic medium (O.M.). VPA promotes chromosomal remodeling and maintains acetylated histones as an "open form" of the chromatin structure by acting as an inhibitor of HDAC.

Meanwhile, in previous studies, ALK5i II was used as a TGF-β R inhibitor in direct conversion, whereby ALK5i II induced fibroblasts to exhibit osteoblast phenotypes with remarkable abilities [62]. Among various ALK5 inhibitors, ALK5i II exhibited the highest inhibition of smad2/3 signaling and induced osteoblastic conversion at the highest efficiency. Previously, it was shown that a TGF-β R inhibitor substituted transcription factors, such as Oct4 or Sox2 in the induction of reprogramming and maintenance of pluripotency [63,64]. Treatment of a TGF-β R inhibitor resulted in an 8-fold increase in the efficiency of the direct conversion of fibroblast into cardiomyocytes induced by cardiomyocyte-specific reprogramming factors [65,66]. A TGF-β R inhibitor was also used as an essential component when tested as a small molecule in the induction of direct conversion of fibroblasts into neural cells [67,68] and cardiomyocytes [69]. It is understood that osteoblasts and osteocytes produce TGF-β, but its roles in osteogenesis is more complicated. It was demonstrated that the TGF-β signal enhances osteoblast differentiation at early stages, whereas at later stages of differentiation, it inhibits proliferation and mineralization of osteoblasts [70]. Other reports have revealed that TGF-β may either stimulate or inhibit the differentiation of osteoblasts as a function of the composition, concentration, density, and differentiation stage of the cells [71,72].

Herein, we employed small molecule VPA, a HDAC inhibitor, in combination with a TGF-β R inhibitor, ALK5i II, for cell fate conversion to efficiently reprogram fibroblasts into osteoblasts. Simultaneous treatment demonstrated a synergistic effect on the direct conversion of somatic cells to osteogenic lineage. It is anticipated that the addition of other small molecules, transcription factors, or supplements may further elevate the expression levels of osteoblast-specific genes and promote the direct conversion efficiency. The generation of functional osteoblasts from human somatic cells could provide an alternative means of bone regenerative therapy for bone disorders such as osteoporosis. The process is attractive because of its advantages, that is, it is a highly efficient conversion step for the production of bone matrix and promoting bone tissue regeneration, and additionally, it is a transgene-free method. Further investigation of the VPA mechanism associated with histone acetylation and the promotion of direct reprogramming efficiency could support the findings of our study. It is anticipated that these results may be beneficial in providing a safer approach and higher reprogramming efficiency for practical use in human therapies.

Author Contributions: H.C. and J.L. collected data and evidence; H.H.P. and J.H.P. conceived and designed the study; H.H.P. and J.H.P. wrote the manuscript; H.C. and J.L. drew the figures; H.H.P. and J.H.P. directed and validated the data analysis. All authors have read and agreed to the published version of the manuscript.

Funding: This work was supported by the Korea Evaluation Institute of Industrial Technology (KEIT) grant funded by the Korea government (MSIT) (No. 20008546). Additionally, this work was also supported by the Bio & Medical Technology Development Program of the National Research Foundation (NRF) funded by Korean Government (Ministry of Science and ICT) (No. 2017M3A9C6031798 and 2016M3A9C6917402).

Conflicts of Interest: The authors declare no conflict of interest.

References

1. Boulikas, T. Putative nuclear localization signals (NLS) in protein transcription factors. *J. Cell. Biochem.* **1994**, *55*, 32–58. [CrossRef] [PubMed]
2. Latchman, D.S. Transcription factors: An overview. *Int. J. Biochem. Cell Biol.* **1997**, *29*, 1305–1312. [CrossRef]
3. Takahashi, K.; Tanabe, K.; Ohnuki, M.; Narita, M.; Ichisaka, T.; Tomoda, K.; Yamanaka, S. Induction of pluripotent stem cells from adult human fibroblasts by defined factors. *Cell* **2007**, *131*, 861–872. [CrossRef] [PubMed]
4. Takahashi, K.; Yamanaka, S. Induction of pluripotent stem cells from mouse embryonic and adult fibroblast cultures by defined factors. *Cell* **2006**, *126*, 663–676. [CrossRef] [PubMed]
5. Zhou, Q.; Melton, D.A. Extreme makeover: Converting one cell into another. *Cell Stem Cell* **2008**, *3*, 382–388. [CrossRef] [PubMed]
6. Ieda, M.; Fu, J.-D.; Delgado-Olguin, P.; Vedantham, V.; Hayashi, Y.; Bruneau, B.G.; Srivastava, D. Direct reprogramming of fibroblasts into functional cardiomyocytes by defined factors. *Cell* **2010**, *142*, 375–386. [CrossRef] [PubMed]
7. Miyamoto, K.; Akiyama, M.; Tamura, F.; Isomi, M.; Yamakawa, H.; Sadahiro, T.; Muraoka, N.; Kojima, H.; Haginiwa, S.; Kurotsu, S. Direct in vivo reprogramming with Sendai virus vectors improves cardiac function after myocardial infarction. *Cell Stem Cell* **2018**, *22*, 91–103. [CrossRef]
8. Pang, Z.P.; Yang, N.; Vierbuchen, T.; Ostermeier, A.; Fuentes, D.R.; Yang, T.Q.; Citri, A.; Sebastiano, V.; Marro, S.; Südhof, T.C. Induction of human neuronal cells by defined transcription factors. *Nature* **2011**, *476*, 220–223. [CrossRef]
9. Thier, M.; Wörsdörfer, P.; Lakes, Y.B.; Gorris, R.; Herms, S.; Opitz, T.; Seiferling, D.; Quandel, T.; Hoffmann, P.; Nöthen, M.M. Direct conversion of fibroblasts into stably expandable neural stem cells. *Cell Stem Cell* **2012**, *10*, 473–479. [CrossRef]
10. Vierbuchen, T.; Ostermeier, A.; Pang, Z.P.; Kokubu, Y.; Südhof, T.C.; Wernig, M. Direct conversion of fibroblasts to functional neurons by defined factors. *Nature* **2010**, *463*, 1035–1041. [CrossRef]
11. Xiao, D.; Liu, X.; Zhang, M.; Zou, M.; Deng, Q.; Sun, D.; Bian, X.; Cai, Y.; Guo, Y.; Liu, S. Direct reprogramming of fibroblasts into neural stem cells by single non-neural progenitor transcription factor Ptf1a. *Nat. Commun.* **2018**, *9*, 1–19. [CrossRef] [PubMed]
12. Hiramatsu, K.; Sasagawa, S.; Outani, H.; Nakagawa, K.; Yoshikawa, H.; Tsumaki, N. Generation of hyaline cartilaginous tissue from mouse adult dermal fibroblast culture by defined factors. *J. Clin. Investig.* **2011**, *121*, 640–657. [CrossRef] [PubMed]
13. Shi, J.-W.; Zhang, T.-T.; Liu, W.; Yang, J.; Lin, X.-L.; Jia, J.-S.; Shen, H.-F.; Wang, S.-C.; Li, J.; Zhao, W.-T.; et al. Direct conversion of pig fibroblasts to chondrocyte-like cells by c-Myc. *Cell Death Discov.* **2019**, *5*, 55. [CrossRef] [PubMed]
14. Wang, Y.; Wu, M.-H.; Cheung, M.P.L.; Sham, M.H.; Akiyama, H.; Chan, D.; Cheah, K.S.; Cheung, M. Reprogramming of dermal fibroblasts into osteo-chondrogenic cells with elevated osteogenic potency by defined transcription factors. *Stem Cell Rep.* **2017**, *8*, 1587–1599. [CrossRef] [PubMed]
15. Chen, G.; Guo, Y.e.; Li, C.; Li, S.; Wan, X. Small Molecules that Promote Self-Renewal of Stem Cells and Somatic Cell Reprogramming. *Stem Cell Rev. Rep.* **2020**, *16*, 511–523. [CrossRef]
16. Chen, S.; Do, J.T.; Zhang, Q.; Yao, S.; Yan, F.; Peters, E.C.; Schöler, H.R.; Schultz, P.G.; Ding, S. Self-renewal of embryonic stem cells by a small molecule. *Proc. Natl. Acad. Sci. USA* **2006**, *103*, 17266–17271. [CrossRef]
17. Fang, L.; Zhu, Q.; Neuenschwander, M.; Specker, E.; Wulf-Goldenberg, A.; Weis, W.I.; Von Kries, J.P.; Birchmeier, W. A small-molecule antagonist of the β-catenin/TCF4 interaction blocks the self-renewal of cancer stem cells and suppresses tumorigenesis. *Cancer Res.* **2016**, *76*, 891–901. [CrossRef]

18. Tsutsui, H.; Valamehr, B.; Hindoyan, A.; Qiao, R.; Ding, X.; Guo, S.; Witte, O.N.; Liu, X.; Ho, C.-M.; Wu, H. An optimized small molecule inhibitor cocktail supports long-term maintenance of human embryonic stem cells. *Nat. Commun.* **2011**, *2*, 1–8. [CrossRef]
19. Wilkinson, A.C.; Igarashi, K.J.; Nakauchi, H. Haematopoietic stem cell self-renewal in vivo and ex vivo. *Nat. Rev. Genet.* **2020**, *21*, 541–554. [CrossRef]
20. Chen, S.; Borowiak, M.; Fox, J.L.; Maehr, R.; Osafune, K.; Davidow, L.; Lam, K.; Peng, L.F.; Schreiber, S.L.; Rubin, L.L. A small molecule that directs differentiation of human ESCs into the pancreatic lineage. *Nat. Chem. Biol.* **2009**, *5*, 258–265. [CrossRef]
21. Cui, Z.-K.; Sun, J.A.; Baljon, J.J.; Fan, J.; Kim, S.; Wu, B.M.; Aghaloo, T.; Lee, M. Simultaneous delivery of hydrophobic small molecules and siRNA using Sterosomes to direct mesenchymal stem cell differentiation for bone repair. *Acta Biomater.* **2017**, *58*, 214–224. [CrossRef] [PubMed]
22. Kanke, K.; Masaki, H.; Saito, T.; Komiyama, Y.; Hojo, H.; Nakauchi, H.; Lichtler, A.C.; Takato, T.; Chung, U.-I.; Ohba, S. Stepwise differentiation of pluripotent stem cells into osteoblasts using four small molecules under serum-free and feeder-free conditions. *Stem Cell Rep.* **2014**, *2*, 751–760. [CrossRef] [PubMed]
23. Olivier, E.N.; Marenah, L.; McCahill, A.; Condie, A.; Cowan, S.; Mountford, J.C. High-efficiency serum-free feeder-free erythroid differentiation of human pluripotent stem cells using small molecules. *Stem Cells Transl. Med.* **2016**, *5*, 1394–1405. [CrossRef] [PubMed]
24. Zhu, S.; Wurdak, H.; Wang, J.; Lyssiotis, C.A.; Peters, E.C.; Cho, C.Y.; Wu, X.; Schultz, P.G. A small molecule primes embryonic stem cells for differentiation. *Cell Stem Cell* **2009**, *4*, 416–426. [CrossRef] [PubMed]
25. Hou, P.; Li, Y.; Zhang, X.; Liu, C.; Guan, J.; Li, H.; Zhao, T.; Ye, J.; Yang, W.; Liu, K.; et al. Pluripotent Stem Cells Induced from Mouse Somatic Cells by Small-Molecule Compounds. *Science* **2013**, *341*, 651–654. [CrossRef] [PubMed]
26. Huangfu, D.; Maehr, R.; Guo, W.; Eijkelenboom, A.; Snitow, M.; Chen, A.E.; Melton, D.A. Induction of pluripotent stem cells by defined factors is greatly improved by small-molecule compounds. *Nat. Biotechnol.* **2008**, *26*, 795–797. [CrossRef] [PubMed]
27. Huangfu, D.; Osafune, K.; Maehr, R.; Guo, W.; Eijkelenboom, A.; Chen, S.; Muhlestein, W.; Melton, D.A. Induction of pluripotent stem cells from primary human fibroblasts with only Oct4 and Sox2. *Nat. Biotechnol.* **2008**, *26*, 1269–1275. [CrossRef]
28. Lin, T.; Ambasudhan, R.; Yuan, X.; Li, W.; Hilcove, S.; Abujarour, R.; Lin, X.; Hahm, H.S.; Hao, E.; Hayek, A.; et al. A chemical platform for improved induction of human iPSCs. *Nat. Methods* **2009**, *6*, 805–808. [CrossRef]
29. Zheng, J.; Choi, K.-A.; Kang, P.J.; Hyeon, S.; Kwon, S.; Moon, J.-H.; Hwang, I.; Kim, Y.I.; Kim, Y.S.; Yoon, B.S.; et al. A combination of small molecules directly reprograms mouse fibroblasts into neural stem cells. *Biochem. Biophys. Res. Commun.* **2016**, *476*, 42–48. [CrossRef]
30. Cao, N.; Huang, Y.; Zheng, J.; Spencer, C.I.; Zhang, Y.; Fu, J.-D.; Nie, B.; Xie, M.; Zhang, M.; Wang, H.; et al. Conversion of human fibroblasts into functional cardiomyocytes by small molecules. *Science* **2016**, *352*, 1216–1220. [CrossRef]
31. Ladewig, J.; Mertens, J.; Kesavan, J.; Doerr, J.; Poppe, D.; Glaue, F.; Herms, S.; Wernet, P.; Kögler, G.; Müller, F.-J.; et al. Small molecules enable highly efficient neuronal conversion of human fibroblasts. *Nat. Methods* **2012**, *9*, 575–578. [CrossRef] [PubMed]
32. Wang, H.; Cao, N.; Spencer, C.I.; Nie, B.; Ma, T.; Xu, T.; Zhang, Y.; Wang, X.; Srivastava, D.; Ding, S. Small Molecules Enable Cardiac Reprogramming of Mouse Fibroblasts with a Single Factor, Oct4. *Cell Rep.* **2014**, *6*, 951–960. [CrossRef] [PubMed]
33. Chang, J.W.; Moellering, R.E. No Bones About It: Small Molecules for Bone Regeneration. *Cell Chem. Biol.* **2019**, *26*, 911–912. [CrossRef]
34. Lo, K.W.-H.; Kan, H.M.; Ashe, K.M.; Laurencin, C.T. The small molecule PKA-specific cyclic AMP analogue as an inducer of osteoblast-like cells differentiation and mineralization. *J. Tissue Eng. Regen. Med.* **2012**, *6*, 40–48. [CrossRef] [PubMed]
35. Shi, A.; Heinayati, A.; Bao, D.; Liu, H.; Ding, X.; Tong, X.; Wang, L.; Wang, B.; Qin, H. Small molecule inhibitor of TGF-β signaling enables robust osteogenesis of autologous GMSCs to successfully repair minipig severe maxillofacial bone defects. *Stem Cell Res. Ther.* **2019**, *10*, 172. [CrossRef] [PubMed]
36. Wu, X.; Ding, S.; Ding, Q.; Gray, N.S.; Schultz, P.G. A Small Molecule with Osteogenesis-Inducing Activity in Multipotent Mesenchymal Progenitor Cells. *J. Am. Chem. Soc.* **2002**, *124*, 14520–14521. [CrossRef] [PubMed]

37. Almalki, S.G.; Agrawal, D.K. Key transcription factors in the differentiation of mesenchymal stem cells. *Differentiation* **2016**, *92*, 41–51. [CrossRef] [PubMed]
38. Pittenger, M.F.; Mackay, A.M.; Beck, S.C.; Jaiswal, R.K.; Douglas, R.; Mosca, J.D.; Moorman, M.A.; Simonetti, D.W.; Craig, S.; Marshak, D.R. Multilineage potential of adult human mesenchymal stem cells. *Science* **1999**, *284*, 143–147. [CrossRef]
39. Yamamoto, K.; Kishida, T.; Sato, Y.; Nishioka, K.; Ejima, A.; Fujiwara, H.; Kubo, T.; Yamamoto, T.; Kanamura, N.; Mazda, O. Direct conversion of human fibroblasts into functional osteoblasts by defined factors. *Proc. Natl. Acad. Sci. USA* **2015**, *112*, 6152–6157. [CrossRef]
40. Komori, T. Regulation of proliferation, differentiation and functions of osteoblasts by Runx2. *Int. J. Mol. Sci.* **2019**, *20*, 1694. [CrossRef]
41. Liu, Z.; Yao, X.; Yan, G.; Xu, Y.; Yan, J.; Zou, W.; Wang, G. Mediator MED23 cooperates with RUNX2 to drive osteoblast differentiation and bone development. *Nat. Commun.* **2016**, *7*, 1–11. [CrossRef] [PubMed]
42. Han, Y.; Kim, Y.-M.; Kim, H.S.; Lee, K.Y. Melatonin promotes osteoblast differentiation by regulating Osterix protein stability and expression. *Sci. Rep.* **2017**, *7*, 1–11. [CrossRef] [PubMed]
43. Nakashima, K.; Zhou, X.; Kunkel, G.; Zhang, Z.; Deng, J.M.; Behringer, R.R.; De Crombrugghe, B. The novel zinc finger-containing transcription factor osterix is required for osteoblast differentiation and bone formation. *Cell* **2002**, *108*, 17–29. [CrossRef]
44. Ju, H.; Lee, S.; Lee, J.; Ghil, S. Necdin modulates osteogenic cell differentiation by regulating Dlx5 and MAGE-D1. *Biochem. Biophys. Res. Commun.* **2017**, *489*, 109–115. [CrossRef] [PubMed]
45. Lee, K.-M.; Park, K.H.; Hwang, J.S.; Lee, M.; Yoon, D.S.; Ryu, H.A.; Jung, H.S.; Park, K.W.; Kim, J.; Park, S.W. Inhibition of STAT5A promotes osteogenesis by DLX5 regulation. *Cell Death Dis.* **2018**, *9*, 1–13. [CrossRef] [PubMed]
46. Rachner, T.D.; Khosla, S.; Hofbauer, L.C. Osteoporosis: Now and the future. *Lancet* **2011**, *377*, 1276–1287. [CrossRef]
47. Buckle, C.H.; De Leenheer, E.; Lawson, M.A.; Yong, K.; Rabin, N.; Perry, M.; Vanderkerken, K.; Croucher, P.I. Soluble rank ligand produced by myeloma cells causes generalised bone loss in multiple myeloma. *PLoS ONE* **2012**, *7*, e41127. [CrossRef]
48. Ahmed, M.F.; El-Sayed, A.K.; Chen, H.; Zhao, R.; Jin, K.; Zuo, Q.; Zhang, Y.; Li, B. Direct conversion of mouse embryonic fibroblast to osteoblast cells using hLMP-3 with Yamanaka factors. *Int. J. Biochem. Cell Biol.* **2019**, *106*, 84–95. [CrossRef]
49. Duan, Q.; Li, S.; Wen, X.; Sunnassee, G.; Chen, J.; Tan, S.; Guo, Y. Valproic Acid Enhances Reprogramming Efficiency and Neuronal Differentiation on Small Molecules Staged-Induction Neural Stem Cells: Suggested Role of mTOR Signaling. *Front. Neurosci.* **2019**, *13*. [CrossRef]
50. Phiel, C.J.; Zhang, F.; Huang, E.Y.; Guenther, M.G.; Lazar, M.A.; Klein, P.S. Histone deacetylase is a direct target of valproic acid, a potent anticonvulsant, mood stabilizer, and teratogen. *J. Biol. Chem.* **2001**, *276*, 36734–36741. [CrossRef]
51. Zhai, Y.; Chen, X.; Yu, D.; Li, T.; Cui, J.; Wang, G.; Hu, J.-F.; Li, W. Histone deacetylase inhibitor valproic acid promotes the induction of pluripotency in mouse fibroblasts by suppressing reprogramming-induced senescence stress. *Exp. Cell Res.* **2015**, *337*, 61–67. [CrossRef] [PubMed]
52. Cedar, H.; Bergman, Y. Linking DNA methylation and histone modification: Patterns and paradigms. *Nat. Rev. Genet.* **2009**, *10*, 295–304. [CrossRef]
53. Li, B.; Carey, M.; Workman, J.L. The role of chromatin during transcription. *Cell* **2007**, *128*, 707–719. [CrossRef] [PubMed]
54. Li, E. Chromatin modification and epigenetic reprogramming in mammalian development. *Nat. Rev. Genet.* **2002**, *3*, 662–673. [CrossRef] [PubMed]
55. Shogren-Knaak, M.; Ishii, H.; Sun, J.-M.; Pazin, M.J.; Davie, J.R.; Peterson, C.L. Histone H4-K16 acetylation controls chromatin structure and protein interactions. *Science* **2006**, *311*, 844–847. [CrossRef] [PubMed]
56. Selokar, N.L.; St. John, L.; Revay, T.; King, W.A.; Singla, S.K.; Madan, P. Effect of histone deacetylase inhibitor valproic acid treatment on donor cell growth characteristics, cell cycle arrest, apoptosis, and handmade cloned bovine embryo production efficiency. *Cell. Reprogramming (Former. "Cloning Stem Cells")* **2013**, *15*, 531–542. [CrossRef]

57. Hao, Y.; Creson, T.; Zhang, L.; Li, P.; Du, F.; Yuan, P.; Gould, T.D.; Manji, H.K.; Chen, G. Mood stabilizer valproate promotes ERK pathway-dependent cortical neuronal growth and neurogenesis. *J. Neurosci.* **2004**, *24*, 6590–6599. [CrossRef]
58. Ni, L.; Wang, L.; Yao, C.; Ni, Z.; Liu, F.; Gong, C.; Zhu, X.; Yan, X.; Watowich, S.S.; Lee, D.A. The histone deacetylase inhibitor valproic acid inhibits NKG2D expression in natural killer cells through suppression of STAT3 and HDAC3. *Sci. Rep.* **2017**, *7*, 45266. [CrossRef]
59. Akshaya, N.; Prasith, P.; Abinaya, B.; Ashwin, B.; Chandran, S.V.; Selvamurugan, N. Valproic acid, A Potential Inducer of Osteogenesis in Mouse Mesenchymal Stem Cells. *Curr. Mol. Pharmacol.* **2020**. [CrossRef]
60. Zhou, D.; Chen, Y.X.; Yin, J.H.; Tao, S.C.; Guo, S.C.; Wei, Z.Y.; Feng, Y.; Zhang, C.Q. Valproic acid prevents glucocorticoid-induced osteonecrosis of the femoral head of rats. *Int. J. Mol. Med.* **2018**, *41*, 3433–3447. [CrossRef]
61. Kang, H.; Shih, Y.-R.V.; Nakasaki, M.; Kabra, H.; Varghese, S. Small molecule–driven direct conversion of human pluripotent stem cells into functional osteoblasts. *Sci. Adv.* **2016**, *2*, e1600691. [CrossRef]
62. Yamamoto, K.; Kishida, T.; Nakai, K.; Sato, Y.; Kotani, S.-I.; Nishizawa, Y.; Yamamoto, T.; Kanamura, N.; Mazda, O. Direct phenotypic conversion of human fibroblasts into functional osteoblasts triggered by a blockade of the transforming growth factor-β signal. *Sci. Rep.* **2018**, *8*, 1–11. [CrossRef]
63. Ichida, J.K.; Blanchard, J.; Lam, K.; Son, E.Y.; Chung, J.E.; Egli, D.; Loh, K.M.; Carter, A.C.; Di Giorgio, F.P.; Koszka, K. A small-molecule inhibitor of Tgf-β signaling replaces Sox2 in reprogramming by inducing Nanog. *Cell Stem Cell* **2009**, *5*, 491–503. [CrossRef]
64. Tan, F.; Qian, C.; Tang, K.; Abd-Allah, S.M.; Jing, N. Inhibition of transforming growth factor β (TGF-β) signaling can substitute for Oct4 protein in reprogramming and maintain pluripotency. *J. Biol. Chem.* **2015**, *290*, 4500–4511. [CrossRef]
65. Ifkovits, J.L.; Addis, R.C.; Epstein, J.A.; Gearhart, J.D. Inhibition of TGFβ signaling increases direct conversion of fibroblasts to induced cardiomyocytes. *PLoS ONE* **2014**, *9*, e89678. [CrossRef] [PubMed]
66. Mohamed, T.M.; Stone, N.R.; Berry, E.C.; Radzinsky, E.; Huang, Y.; Pratt, K.; Ang, Y.-S.; Yu, P.; Wang, H.; Tang, S. Chemical enhancement of in vitro and in vivo direct cardiac reprogramming. *Circulation* **2017**, *135*, 978–995. [CrossRef]
67. Hu, W.; Qiu, B.; Guan, W.; Wang, Q.; Wang, M.; Li, W.; Gao, L.; Shen, L.; Huang, Y.; Xie, G. Direct conversion of normal and Alzheimer's disease human fibroblasts into neuronal cells by small molecules. *Cell Stem Cell* **2015**, *17*, 204–212. [CrossRef] [PubMed]
68. Li, X.; Zuo, X.; Jing, J.; Ma, Y.; Wang, J.; Liu, D.; Zhu, J.; Du, X.; Xiong, L.; Du, Y. Small-molecule-driven direct reprogramming of mouse fibroblasts into functional neurons. *Cell Stem Cell* **2015**, *17*, 195–203. [CrossRef] [PubMed]
69. Fu, Y.; Huang, C.; Xu, X.; Gu, H.; Ye, Y.; Jiang, C.; Qiu, Z.; Xie, X. Direct reprogramming of mouse fibroblasts into cardiomyocytes with chemical cocktails. *Cell Res.* **2015**, *25*, 1013–1024. [CrossRef] [PubMed]
70. Julia, X.Y.; Li, T.H. Distinct biological effects of different nanoparticles commonly used in cosmetics and medicine coatings. *Cell Biosci.* **2011**, *1*, 1–9.
71. de Gorter, D.J.; van Dinther, M.; Korchynskyi, O.; ten Dijke, P. Biphasic effects of transforming growth factor β on bone morphogenetic protein–induced osteoblast differentiation. *J. Bone Miner. Res.* **2011**, *26*, 1178–1187. [CrossRef] [PubMed]
72. Suzuki, E.; Ochiai-Shino, H.; Aoki, H.; Onodera, S.; Saito, A.; Saito, A.; Azuma, T. Akt activation is required for TGF-β1-induced osteoblast differentiation of MC3T3-E1 pre-osteoblasts. *PLoS ONE* **2014**, *9*, e112566. [CrossRef] [PubMed]